



HAL
open science

Carbon monoxide substitutions by trimethyl phosphite in diiron dithiolate complex Fe-Fe bond cleavage, selectivity of the substitutions, crystal structures and electrochemical studies

N.B. Makouf, H.B. Mousser, A. Darchen, A. Mousser

► To cite this version:

N.B. Makouf, H.B. Mousser, A. Darchen, A. Mousser. Carbon monoxide substitutions by trimethyl phosphite in diiron dithiolate complex Fe-Fe bond cleavage, selectivity of the substitutions, crystal structures and electrochemical studies. *Journal of Organometallic Chemistry*, 2018, 866, pp.35-42. 10.1016/j.jorganchem.2018.04.005 . hal-01809155

HAL Id: hal-01809155

<https://univ-rennes.hal.science/hal-01809155>

Submitted on 20 Jun 2018

HAL is a multi-disciplinary open access archive for the deposit and dissemination of scientific research documents, whether they are published or not. The documents may come from teaching and research institutions in France or abroad, or from public or private research centers.

L'archive ouverte pluridisciplinaire **HAL**, est destinée au dépôt et à la diffusion de documents scientifiques de niveau recherche, publiés ou non, émanant des établissements d'enseignement et de recherche français ou étrangers, des laboratoires publics ou privés.

1 **Carbon monoxide substitutions by trimethyl phosphite in diiron dithiolate complex: Fe-**
2 **Fe bond cleavage, selectivity of the substitutions, crystal structures and electrochemical**
3 **studies**

4 Naouel Boukrina Makouf¹, Hénia Bouzidi Mousser^{1,2*}, André Darchen³ and Abdelhamid
5 Mousser¹

6 ¹Laboratoire de Physicochimie Analytique et Cristallochimie de Matériaux
7 Organométalliques et Biomoléculaires, Université des Frères Mentouri Constantine 1,
8 Algérie.

9 ²Ecole Normale Supérieure Assia Djebar Constantine, Ville Universitaire Ali Mendjeli
10 Constantine, Algérie.

11 ³UMR CNRS No. 6226, Institut des Sciences Chimiques de Rennes, ENSCR, 11 Allée de
12 Beaulieu, CS 50837, 35708 Rennes Cedex 7, France

13
14 * Corresponding author. Tel.: +213 661 57 58 52

15 E-mail address: bouzidi_henia@yahoo.fr (Hénia Bouzidi Mousser)

16
17 **Abstract**

18
19 The reaction of substitution of carbon monoxide by P(OMe)₃ in the complex (μ -
20 $\eta^2\text{PhC(S)=C(S)PhFe}_2(\text{CO})_6$ **1** under thermal activation afforded two colored compounds: a
21 binuclear disubstituted complex (μ -PhC(S)=C(S)Ph)Fe₂(CO)₄[P(OMe)₃]₂ **2** and a
22 mononuclear iron disubstituted complex ($\eta^2\text{PhC(S)=C(S)PhFe}(\text{CO})[\text{P(OMe)}_3]_2$ **3**. Mass
23 spectrometry, ¹H NMR, IR and electrochemical studies established that two (CO) have been
24 substituted by P(OMe)₃ in complexes **2** and **3**. The X-ray studies show that the two P(OMe)₃

1 ligands are in apical positions in trans of the iron – iron bound of complex **2** and in equatorial
2 positions in complex **3**. However, the substitution reaction of (CO) by P(OMe)₃ in complex **1**
3 under electron transfer catalysis (ETC) led to the monosubstituted compound (μ -
4 PhC(S)=C(S)Ph)Fe₂(CO)₅[P(OMe)₃] **4**.

5
6 *Keywords:* [FeFe] hydrogenase; Carbon monoxide substitution; Diiron hexacarbonyl
7 complex; Thermal activation; Electron transfer catalysis; Single-crystal X-ray study
8

9 **1. Introduction**

10
11 Among vital hydrogenase enzymes, [FeFe] hydrogenases are receiving a special attention,
12 due to their unusual structures and their catalytic power in production of hydrogen. The
13 crystal structure of the [FeFe] hydrogenase was first reported in 1998 by Peters *et al.* [1] and
14 later by Nicolet *et al* [2]. The binuclear complexes of iron whose structures are close to those
15 of the [FeFe] hydrogenase complexes have been known for more than 80 years [3]. Since
16 [FeFe] hydrogenase crystal structure publication [1], some complexes containing a Fe₂S₂
17 core have attracted the interest of chemists [4–8]. These complexes are easily synthesized and
18 have been studied as structural and functional mimics of enzyme active site [9]. The catalytic
19 properties for hydrogen generation by models of [FeFe] hydrogenases can be modified by
20 substitution of one or two (CO) by more donor ligands in order to increase the electron
21 density at the iron atoms enhancing its basicity. This substitution reactions can be carried out
22 under thermal activation [10,11], photochemical activation [12,13] and Electron Transfer
23 Catalysis (ETC) or electrochemical activation [14,15] and is of major importance in
24 organometallic and coordination chemistry in connection with catalytic processes.

1 The carbon monoxide substitution by a ligand L more donor than (CO) has been largely
2 investigated in iron polynuclear complexes [16–27]. Binuclear compounds (μ - η^2 -ROCS)(μ -
3 SMe)Fe₂(CO)₆ [16] and [(μ -RS)₂Fe₂(CO)₆] [25] reacted with P(OMe)₃ under ETC activation
4 to afford monosubstituted compounds firstly and then the disubstituted products [17,18,28].
5 The results are apparently consistent with the empirical rule that one (CO) substitution occurs
6 at each metal centre [29]. However kinetic studies [30] and sequential use of P(OMe)₃ and
7 P(OCD₃)₃ [31] have revealed that the participation of bridging ligands does not be neglected
8 and the second (CO) substitution may be not exclusively on the unsubstituted metal center.
9 Under thermal activation, Lagadec *et al.* [32] studied the (CO) substitution in the binuclear
10 complexes [R1C(S)SR₂]Fe₂(CO)₆ and established that, with ligands such as L = P(OMe)₃,
11 CNR or PPh₂, monosubstituted products were exclusively obtained. For all carbon
12 monoxide substitutions by trimethyl phosphate in diiron hexacarbonyl complexes carried out
13 under thermal or electron transfer catalysis activations [23], the same monosubstitution
14 regioselectivity was observed in each case. Binuclear iron complexes with sulfured organic
15 bridges are generally stable during their thermal reaction with ligands more donor than (CO)
16 [27,33]. Surprisingly, we have observed an unusual Fe-Fe bond cleavage in the complex (μ -
17 η^2 PhC(S)=C(S)Ph)Fe₂(CO)₆ **1** [34] during its thermal reaction with P(OMe)₃.
18 This work is a part of aiming to perform substitution reactions of (CO) by ligands more donor
19 in iron complexes having close resemblance to the diiron unit of the [FeFe] hydrogenase
20 under thermal and ETC activations. In complex **1** when P(OMe)₃ was used in substitution
21 under thermal activation two complexes **2** and **3** were obtained (Scheme 1). The X-ray studies
22 show that the two P(OMe)₃ are in apical positions in trans of the iron – iron bound in complex
23 **2** and in equatorial positions in complex **3**. However the ETC substitution reaction led to the
24 monosubstituted compound **4** (Scheme 1) according with spectroscopy and electrochemical

1 analysis. In order to understand these exchange ligand reactions, the electrochemical behavior
2 of complexes **1**, **2**, **3** and **4** was investigated and the results are reported here.

3

4 **Scheme 1**

5

6 **2. Experimental**

7

8 *2.1. Physical measurements*

9

10 ¹H NMR spectra were recorded at 89.55 MHz, in CDCl₃ with TMS as internal standard. Mass
11 spectra were recorded with a Varian MAT 311 spectrophotometer at 70 eV at CRMPO
12 (Rennes, France). Elemental analyses were carried out by Service Central d'Analyse
13 (Vernaison, France). The electrochemical experiments were carried out in a three – electrode
14 thermostated cell with a PAR 362 potentiostat coupled to a Kipp and Zonem XY recorder. Pt
15 micro disc and a saturated calomel electrode (SCE) were used as working and reference
16 electrodes, respectively. Diffraction measurements of single crystals of complexes **2** and **3**
17 were made at 293 K on a Kappa CCD diffractometer (Bruker AXS BV, 1997 – 2004)
18 equipped with a graphite monochromatic using Mo K α radiation ($\lambda = 0.71073 \text{ \AA}$). Crystal
19 data collection reduction and refinement were accomplished with COLLECCT (Nonius,
20 1998), SCALEPACK and DENZO [35] programs. The structure was solved by SIR 2002 [36]
21 and refined by using SHELXL-97 [37]. The hydrogen atoms were located in Fourier maps
22 but introduced in calculated positions and treated as riding on their parent C atom, with 0.95
23 (aromatic) and with Uiso(H) = 1.2 Ueq (aromatic C atoms). The molecular graphical was
24 showed with ORTEP – 3 [38] program and material for publication was prepared with
25 WinGX 1.7 software [39,40].

1
2
3
4
5
6
7
8
9
10
11
12
13
14
15
16
17
18
19
20
21
22
23
24
25

2.2. Reagents

The supporting electrolyte Bu_4NBF_4 (Fluka, Purum) was recrystallized in a mixture of methanol and water (1/1), dried at 120°C and used at 0.1 M concentration. Diiron nonacarbonyl (Strem Chemical, 99%), trimethylphosphite (Fluka, Purum, 97%) and diphenylacetylene (Aldrich, 99%) were used as received. Toluene, petroleum ether, ethanol, CH_2Cl_2 and DMF (SDS, analytical grade) were stored over 4 Å molecular sieves before use.

2.3. Preparations

2.3.1. Reaction of $(\mu\text{-}\eta^2\text{PhC(S)=C(S)Ph})\text{Fe}_2(\text{CO})_6$ **1** with P(OMe)_3 under thermal activation

Diiron hexacarbonyl compound **1** was prepared according to the literature [34]. P(OMe)_3 (5 mmol) was added to compound **1** (1.5 mmol) in dry toluene (20 ml). The mixture, in the dark and under nitrogen, was heated at 45°C for 1 h. The progress of the reaction was followed by thin layer chromatography. The reaction products were separated by chromatography on thin layer of silica gel and elution with petroleum ether. The isolated complexes were: **2** (30%) and **3** (25%). They were purified by crystallization from ethanol solution. All yields are based on $(\text{Ph}(\text{CS})_2\text{Ph})\text{Fe}_2(\text{CO})_6$.

2.3.1.1. Complex **2**. $(\mu\text{-PhC(S)=C(S)Ph})\text{Fe}_2(\text{CO})_4[\text{P(OMe)}_3]_2$, m.p. 137°C . ^1H NMR δ : 7.2(m) ppm. IR(KBr): ν CO = 1920; 1930; 1950; 2020 cm^{-1} . Mass spectrum: M^+ found 685.9329; M^+ calc. 685.9348.

1 2.3.1.2. *Complex 3.* ($\eta^2\text{PhC(S)=C(S)Ph}$) $\text{Fe(CO)[P(OMe)}_3\text{]}_2$, m.p. 148°C. $^1\text{H NMR } \delta$: 7.2(m)
2 ppm. IR(KBr): ν CO = 1950 cm^{-1} . Mass spectrum: M^+ found 574.0071; M^+ calc. 574.0100.

3

4 2.3.2. *Reaction of (μ - $\eta^2\text{PhC(S)=C(S)Ph}$) $\text{Fe}_2(\text{CO})_6$ **1** with P(OMe)_3 under ETC*

5 P(OMe)_3 (5 mmol) was added to complex diiron hexacarbonyl **1** [34] (0.38 mmol) in CH_2Cl_2
6 0.1 M $\text{Bu}_4\text{N}^+\text{BF}_4^-$ (25 ml), in the dark and under nitrogen. The electrolysis was carried out
7 by holding the potential at -0.85 V *versus* SCE and was stopped when the electrolyzing
8 current dropped sharply and the change in current reached minimal. After filtration,
9 evaporation of the solvent and chromatography on silica gel the complex **4** (70%) was
10 isolated and was purified by crystallization from ethanol solution.

11

12 2.3.2.1. *Complex 4.* (μ - PhC(S)=C(S)Ph) $\text{Fe}_2(\text{CO})_5\text{P(OMe)}_3$, m.p. 101°C. $^1\text{H NMR } \delta$: 7.2(m)
13 ppm. IR(C_2Cl_4): ν CO = 1950; 1990; 2000; 2060 cm^{-1} . Mass spectrum: M^+ found 589.90017;
14 M^+ calc. 589.90084.

15

16 3. Results and discussion

17

18 3.1. *Thermal reaction of **1** with P(OMe)_3*

19

20 Under thermal activation an excess of P(OMe)_3 reacted with $\text{Ph(CS)}_2\text{PhFe}_2(\text{CO})_6$ **1** and
21 afforded two colored compounds: **2** (30 %) and **3** (25 %). Spectroscopic (Mass, $^1\text{HNMR}$, IR)
22 analysis showed that complex **2** was a disubstituted binuclear compound. The IR spectrum of
23 **2** on KBr pellet displayed intense bands between 1920 and 2020 cm^{-1} which were assigned to
24 the terminal carbonyl coordinated to iron atoms. Mass spectrometry confirmed the presence of
25 two P(OMe)_3 in the compound **2**. The aromatic proton resonance was assigned to the complex

1 multiplet centered at δ 7.2 ppm. Compound **3** was a mononuclear complex carrying two
2 $P(O\text{Me})_3$ ligands. The formation of complex **3** involves the occurrence of a fragmentation on
3 the iron carbonyl complex **1** during its thermal reaction with $P(O\text{Me})_3$. In order to understand
4 this reaction, we investigated the cyclic voltammetry of complex **1** in the presence of
5 $P(O\text{Me})_3$ ligand. ~~and the of complex **1** was performed.~~

6 3.2. Reaction of **1** with $P(O\text{Me})_3$ under ETC

7 8 3.2.1. Cyclic voltammetry of complex **1**

9
10 In CH_2Cl_2 , at room temperature, complex **1** underwent one two-electron reversible reduction
11 step and the reduction potential was observed at - 0.99 V *versus* SCE (Fig.1). However, the
12 lability of **1** may be disclosed in the presence of a donor ligand. When a ligand $P(O\text{Me})_3$ was
13 added into solution of **1**, the cyclic voltammogram (Fig.1) showed the typical behavior of a
14 (CO) substitution by $P(O\text{Me})_3$ catalyzed by electron transfer occurring at the cathode surface
15 [41, 42]. The cathodic peak C1 ($E_{pc} = - 0.90$ V *versus* SCE) of **1** decreased while a peak C2,
16 corresponding to the superposition of two peaks, appeared at more negative potential ($E_{pc} = -$
17 1.30 V *versus* SCE) and indicated the formation of mono and disubstituted complexes.

18 **Fig. 1**

19 20 3.2.2. Electrolysis of complex **1** in the presence of $P(O\text{Me})_3$

21
22 The addition of an excess of $P(O\text{Me})_3$ to a solution of **1** under ETC led to the monosubstituted
23 complex **4**. The electrolysis (45 min) was carried out at - 0.85 V *versus* SCE, in the dark and
24 under nitrogen atmosphere. The mixture was treated and separated by chromatography on

1 silica gel. No fragmentation of the iron carbonyl complex **1** was observed and the expected
2 monosubstituted complex **4** (70%) was isolated.

3

4 3.2.3. Voltammetric studies

5

6 To understand the mechanism substitution reaction, voltammetric studies of the complexes **2**,
7 **3** and **4** were performed.

8 a. Cyclic voltammetry of complex **2**

9 Under N₂ atmosphere complex **2** was reduced in CH₂Cl₂ solution in a single chemically
10 reversible two–electron step (C₁/A₁) at - 1.5 V versus SCE (Fig.2). These observations
11 indicate that the bielectronic reduction of complex **2** is made according to a mechanism ECE
12 where the chemical step may be the Fe-S bond cleavage leading to the anion **2**²⁻ according to
13 the described reduction of (μ²-SPhS-)Fe₂(CO)₆ with 2 equiv of electrons [43]. The chemical
14 step of this mechanism is also reversible.



16

17 Under CO atmosphere, the dianion **2**²⁻ is not stable. The coordination of (CO) induced
18 replacement of the two P(OMe)₃ ligands and at the reverse scan, voltammogram revealed the
19 formation of the hexacarbonyl complex **1** (Fig.2, system C₂/A₂). At more negative potentials
20 an insertion of (CO) on the dianion **2**²⁻ can lead, after Fe-Fe bond cleavage, to an
21 heptacarbonyl complex **5** (Scheme 2) whose oxidation is observed at -0.5 V *versus* SCE (peak
22 A₃) according to an ECEC mechanism.

1

2 **Fig. 2**

3

4 **Scheme 2**

5

6 *b. Cyclic voltammetry of complex 3*

7 Under N₂ atmosphere complex **3** was reduced in CH₂Cl₂ solution in a single chemically
8 reversible two–electron step (Fig.3, system C₁/A₁) at - 1.25 V *versus* SCE in comparison with
9 the intensity of the reduction current of the complex **1**. The obtained dianion **3**²⁻ was also
10 stable and involved an ECE mechanism with a reversible chemical step where the chemical
11 step may be the Fe-S bond cleavage leading to the anion **3**²⁻.

12

13



14

15 Under CO atmosphere, the voltammogram shows a high reactivity of the dianion **3**²⁻. Indeed,
16 during the first potential scan a new reversible system C₂/A₂ appeared at - 0.9 V *versus* SCE
17 assigned to tricarbonyl mononuclear complex **6** (Scheme 3) which oxidizes around -0.5 V
18 *versus* SCE (Fig.3, peak A₃) according to an ECEC mechanism.

19

20 **Fig. 3**21 **Scheme 3**

22

1 *c. Cyclic voltammetry of complex 4*

2

3 Under N₂ atmosphere the binuclear compound **4** was reduced in CH₂Cl₂ solution in a single
 4 chemically reversible two–electron step (Fig.4, peaks C₁ and A₁) observed at - 1.15 V *versus*
 5 SCE (Fig.4) in comparison with the intensity of the reduction current of the complex **1**. These
 6 observations indicate that the dianion **4**²⁻ was stable and involved an ECE mechanism with a
 7 reversible chemical step where the chemical step may be the Fe-S bond cleavage.

8

9



10

11 The difference between the reduction potentials of complexes **1** and **4** is about of 300 mV and
 12 is in agreement with a monosubstitution of (CO) by P(OMe)₃.

13 Under CO atmosphere the voltammogram of **4** (Fig.4) showed that P(OMe)₃ can be replaced
 14 by (CO) after reduction of complex **4** into dianion **4**²⁻. During the reverse scan, two reversible
 15 systems A₂/C₂ and A₃/C₃ were observed at - 0.9 V and - 0.5 *versus* SCE, respectively. A₂/C₂
 16 was attributed to **1**/**1**²⁻ system and A₃/C₃ may be assigned to the system **5**/**5**²⁻ oxidation and
 17 reduction, according to the hypothesis that we have already formulated during the study of
 18 precedent complexes studies under CO atmosphere (Scheme 2).

19

20 **Fig. 4**

21

22 The structures of **2** and **3** were not clearly specified and an X-ray determination was needed to
 23 prove the proposed formulas in order to follow all the discussions on our results. However,

1 the crystal structure of complex **4** could not be determined because of the poor quality of the
2 relevant crystals.

3

4 3.3. X – Ray crystal analysis

5 3.3.1. X – Ray crystal analysis of compound **2**

6

7 Crystals of complex **2** were triclinic with space group P-1. The X – Ray study of **2** established
8 that it was a binuclear disubstituted complex. As expected, the molecular geometry of
9 complex **2** is analogous to that of its parent arene dithiolate diiron complex **1**. The molecular
10 structure (Fig. 5) shows that one CO substitution occurs on each metal center, according to the
11 empirical rule [29]. The two P(OMe)₃ are in apical positions in trans of the iron – iron bound
12 (Fig. 5). The Fe-Fe bond length [2.4797(1) Å] is in accordance with that observed in [Fe₂(μ-
13 btdt)(CO)₄(P(OEt)₃)₂] complex [33] and is slightly shorter than that observed in the starting
14 complex **1** [34]. The average Fe-P distances and Fe-Fe-P angles are 2.1703 Å and 150.275°,
15 respectively and are comparable to those observed for the selenium analogous complexes
16 [44]. The average Fe-S-Fe angle and C-O distances of 65.94° and 1.1469 Å, respectively are
17 in the same ranges of similar complexes [33]. The Fe-S bonds in **2** are slightly longer (ca.
18 0.0137 Å) than that in the unsubstituted compound **1** due to the stronger σ-donor properties of
19 phosphite ligands compared to carbonyl groups [34]. Crystal data collection parameters and
20 some of selected bond lengths and bond angles were given in Tables 1 and 2, respectively. In
21 the crystal packing, the components of the structure are linked via intermolecular C–H...O
22 and C–H...S hydrogen bonds (Table 3) to form a zigzag chain along the *a*-axis (Fig.6).

23

1 **Fig. 5**

2

3 Collection parameters are shown in Table 1, and selected bond distances and angles are
4 tabulated in Table 2.

5

6 **Table 1**

7

8 **Fig.6**

9

10 **Table 2**

11

12 *3.3.2. X – ray crystal analysis of compound 3*

13 Crystals of complex **3** were orthorhombic with space group P_{cab} . The X – Ray study of **3**
14 established that it was a mononuclear disubstituted iron complex with trigonal-bipyramidal
15 geometry. The $[C_6H_5CS]_2$ group was coordinated to the iron atom through the two Fe – S
16 bounds. The Fe – S bond lengths 2.1932(14) Å and 2.1523(13) Å are comparable to those
17 observed for sulfur analogues [45] and were shorter than those obtained in complexes **1** [34]
18 and **2**. The dithio diphenylethylene groups were coordinated to the single iron with the two
19 similar -S-C(Ph) and the mean (1.7315 Å) of the -S-C(Ph) bond lengths was shorter than that
20 observed in complexes **1** [34] and **2**. The P atoms were coordinated in an equatorial position
21 with Fe-P bond lengths [2.1452(14) Å and 2.1220(14) Å] and S-Fe-P angles [117.74(5)°,
22 144.05(5)°, 89.04(5)° and 95.87(5)°] are in accordance with those observed in similar

1 complexes [45]. The coordination of the metal center was completed by one carbonyl in
2 apical position [170.56(16)°]. The Fe–CO bond (1.740(5) Å) is slightly shorter than that
3 observed in the complex **1** [34] and can be due to the π back-donation of the iron atom
4 towards the carbonyl [23]. O2 and C2 atoms of P(OMe)₃ group present a severe disorder. The
5 refined model using constraints corresponds to a distribution of these two atoms with 0.70 and
6 0.60 for O2 and C2 respectively (Fig. 7). Its crystal and collection parameters are shown in
7 Table 1, and selected bond distances and angles are tabulated in Table 2. In the molecular
8 stacking up of the complex **3**, every two molecules are interpenetrated and linked via
9 intermolecular C–H...O hydrogen bond (Table 3), forming a zigzag chain along the *b* axis at
10 $c = 0$ or $c = 1/2$ (Fig. 8). The double bond PhC(S)=C(S)Ph (C5=C6 of 1.3273 (5) Å) in
11 complex **2** is shorter than that observed in complex **3** (C8=C9 of 1.364 (6) Å) and can be
12 explained by a greater steric consideration in the complex **2**.

13

14 **Fig.7**

15

16 **Fig.8**

17

18 **Table 3**

19

20 3.4. *Proposed mechanism for the formation of complexes 2, 3 and 4*

21

22 The formation of **2**, **3** and **4** are summarized in the scheme 4. However the mechanism of the
23 reaction of complex **1** with an excess of P(OMe)₃ could proceed according to a system

1 composed of consecutive and competitive reactions. Thus the monosubstituted complex **4** is
2 firstly formed, whatever the thermal [33] or E.T.C [46] activation. Starting from an excess of
3 the $\text{P}(\text{OMe})_3$, under thermal activation, complex **4** could be involved in two competitive
4 substitution reactions (Scheme 5). The first one would be a (CO) exchange reaction consistent
5 with the empirical rule that one (CO) substitution occurs at each metal center [29] leading to
6 the complex **2**. The second (CO) substitution could occur on the same already substituted iron
7 atom of **2** or **4** leading to a fragmentation resulting from the important steric effect and the
8 resulting high charge density on this iron leading to the complex **3**. $\text{Fe}(\text{CO})_4^{2-}$ fragment could
9 be formed as decomposition product of complexes **2** or **4**.

10

11 **Scheme 4**

12

13 **Scheme 5**

14

15 **4. Conclusion**

16 In this study, we have reported that exchange carbonyl reactions by $\text{P}(\text{OMe})_3$ in complex (μ -
17 $\eta^2\text{PhC}(\text{S})=\text{C}(\text{S})\text{Ph}$) $\text{Fe}_2(\text{CO})_6$ **1** lead to three complexes, depending on the used activation. A
18 binuclear disubstituted complex (μ - $\text{PhC}(\text{S})=\text{C}(\text{S})\text{Ph}$) $\text{Fe}_2(\text{CO})_4[\text{P}(\text{OMe})_3]_2$ and a mononuclear
19 iron disubstituted complex ($\eta^2\text{PhC}(\text{S})=\text{C}(\text{S})\text{Ph}$) $\text{Fe}(\text{CO})[\text{P}(\text{OMe})_3]_2$ were obtained under
20 thermal activation. When using electron transfer catalysis the monosubstituted compound (μ -
21 $\text{PhC}(\text{S})=\text{C}(\text{S})\text{Ph}$) $\text{Fe}_2(\text{CO})_5[\text{P}(\text{OMe})_3]$ was obtained. All the synthesized complexes were
22 characterized by spectroscopic analysis (Mass, ^1H NMR, IR). Cyclic voltammetry of
23 complexes **1-4** were carried out and showed that they underwent in a single chemically
24 reversible two-electron reduction step. Exchange of CO by $\text{P}(\text{OMe})_3$ induced by electron
25 transfer were observed in the complex (μ - $\eta^2\text{PhC}(\text{S})=\text{C}(\text{S})\text{Ph}$) $\text{Fe}_2(\text{CO})_6$. Under CO atmosphere

1 P(OMe)₃ were replaced by CO ligand in a chemical reversible step. The X-ray studies of (μ-
2 PhC(S)=C(S)Ph)Fe₂(CO)₄[P(OMe)₃]₂ and (η²PhC(S)=C(S)Ph)Fe(CO)[P(OMe)₃]₂ were
3 established and showed that the P(OMe)₃ are in apical positions in the binuclear disubstituted
4 complex and are in equatorial positions in the mononuclear iron disubstituted complex.
5 Finally the exchange reaction of carbonyl by P(OMe)₃ in the complex (μ-
6 η²PhC(S)=C(S)Ph)Fe₂(CO)₆ is not selective and the two ways (thermal activation and electron
7 transfer catalysis) did not lead to the same compounds.

8

9 **Formatting of funding sources**

10 This research did not receive any specific grant from funding agencies in the public,
11 commercial, or not-for-profit sectors.

12

13 **Acknowledgements**

14 The authors express their thanks to the Algerian « Ministère de l'Enseignement Supérieur et
15 de la Recherche Scientifique » and the Algerian « Direction Générale de la Recherche
16 Scientifique et du Développement Technologique » for financial support.

17

18 **References**

- 19 [1] J.W. Peters, W.N. Lanzilotta, B.J. Lemon, L.C. Seefeldt, *Science* 282 (1998) 1853–1858.
20 [2] Y. Nicolet, C. Piras, P. Legrand, C.E. Hatchikian, J.C. Fontecilla-Camps, *Structure* 7
21 (1999) 13–23.
22 [3] H. Reihlen, A. Gruhl, G. V. Hessling, *Justus Liebigs Ann. Chem.* 472 (1929) 268–287.
23 [4] B.J. Petro, A.K. Vannucci, L.T. Lockett, C. Mebi, R. Kottani, N.E. Gruhn, G.S. Nichol,
24 P.A.J. Goodyer, D.H. Evans, R.S. Glass, D.L. Lichtenberger, *J. Mol. Struct.* 890 (2008) 281–
25 288.

- 1 [5] X.-F. Liu, *Polyhedron* 119 (2016) 71–76.
- 2 [6] J. Windhager, R. A. Seidel, U. P. Apfel, H. Görls, G. Linti, W. Weigand, *Eur. J. Inorg.*
3 *Chem.* 10 (2008) 2023–2041.
- 4 [7] T. B. Rauchfuss, *Acc. Chem. Res.* 48, 7 (2015) 2107–2116.
- 5 [8] X. Yu, C.-H. Tung, W.G. Wang, M.T. Huynh, D.L. Gray, S. Hammes-Schiffer, T.B.
6 Rauchfuss, *Organometallics* 36 (2017) 2245–2253.
- 7 [9] Y. Si, M. Hu, C. Chen, *CR Chim.* 11 (2008) 932–937.
- 8 [10] A. Rahaman, F.R. Alam, S. Ghosh, D.A. Tocher, M. Haukkae, S.E. Kabir, E.
9 Nordlander, G. Hogarth, *J. Organomet. Chem.* 751 (2014) 326–335.
- 10 [11] J. He, C.-L. Deng, Y. Li, Y.-L. Li, Y. Wu, L.-K. Zou, Ch. Mu, Q. Luo, B. Xie, J. Wei, J.-
11 W. Hu, P.-H. Zhao, W. Zheng, *Organometallics* 36, 7 (2017) 1322–1330.
- 12 [12] B. Pfister, R. Stauber, A. Salzer, *J. Organomet. Chem.* 533 (1997) 131–141.
- 13 [13] P. H. Zhao, D. L. Gray, T. B. Rauchfuss, *Eur. J. Inorg. Chem.* (2016) 2681–2683.
- 14 [14] W. Jiang, Z. Li, X. Zeng, G. Wei, *Asian J. Chem.* 25, 14 (2013) 7655–7659.
- 15 [15] H. Hartmann, B. Sarkar, W. Kaim, J. Fielder, *J. Organomet. Chem.* 687 (2003) 100–107.
- 16 [16] A. Darchen, E. Lhadi, H. Patin, D. Grandjean, A. Mousser, *J. Organomet. Chem.* 385
17 (1990) C4–C8.
- 18 [17] A. Darchen, H. Mousser, H. Patin, *J. Chem. Soc. Chem. Commun.* (1988) 968–970.
- 19 [18] A. Darchen, E. Lhadi, H. Patin. *J. Organomet. Chem.* 259 (1983) 189–206.
- 20 [19] M. Natarajan, I.K. Pandey, S. Kaur-Ghumaan. *Dalton Trans.* DOI:
21 10.1039/C7DT01994G.
- 22 [20] W. Weia, T. Zheng, G. Zhao, G. Zeng, Z. Chi, L. Zhu, *J. Organomet. Chem.* 777, (2015)
23 67–70.

- 1 [21] P. Zhao, X.-Y. Yu, X.-F. Liu, Y.-L. Li, Polyhedron 139 (2018) 116–124.
- 2 [22] Y.-D. Sheng, X.-Y. Yu, X.-F. Liu, Y.-L. Li, Polyhedron 137 (2017) 134–139.
- 3 [23] E. K.Lhadi, C. Mahe, H. Patin, A. Darchen, J. Organomet. Chem. 246, 2 (1983) C61–
4 C64.
- 5 [24] L.-C. Song, W. Gao, X. Luo, Z.-X. Wang, X.-J. Sun, Hai-Bin Song, Organometallics
6 31(2012) 3324–3332.
- 7 [25] D. Seyferth, R.S. Henderson, Li-Cheng Song, G.B. Womack. J. Organomet. Chem. 292
8 (1985) 9–17.
- 9 [26] Y.-L. Li, Z.-Y. Ma, J. He, M.-Y. Hu, P.-H. Zhao. J. Organomet. Chem. 851 (2017) 14–
10 21.
- 11 [27] S. Ghosh, B. E. Sanchez, I. Richards, M. N. Haque, K. B. Holt, M. G. Richmond, G.
12 Hogarth. J. Organomet. Chem. 812 (2016) 274–258.
- 13 [28] H. Patin, A. Le Rouzic, E.K. Lhadi, A. Darchen, A. Mousser, D. Grandjean. J.
14 Organomet. Chem. 375 (1989) 101–114.
- 15 [29] M.I. Bruce, J.G. Matison, B.K. Nicholson, M.L. Williams. J. Organomet. Chem. 236
16 (1982) C57–C60.
- 17 [30] A. Darchen, E. Lhadi, H. Patin. J. Organomet. Chem. 363 (1989) 137–149.
- 18 [31] A. Darchen, E. Lhadi, H. Patin. J. Organomet. Chem. 327 (1987) C37–C40.
- 19 [32] A. Lagadec, B. Misterkiewicz, H. Patin, A. Mousser, J.Y. Le Marouille. J. Organomet.
20 Chem. 315 (1986) 201-210.
- 21 [33] G. Durgaprasad, S.K. Das. J. Organomet. Chem. 717 (2012) 29–40.

- 1 [34] H. Mousser, A. Darchen, A. Mousser. *J. Organomet. Chem.* 695 (2010) 786–791.
- 2 [35] Z. Otwinowski, W. Minor, in: C.W. Carter, R.M. Sweet (Eds.), *Methods in Enzymology.*
3 *Macromolecular Crystallography. Part A, Vol. 276*, Academic Press, New York, 1997, pp.
4 307 – 326.
- 5 [36] M.C. Burla, M. Camalli, B. Carrozzini, G.L. Cascarano, C. Giacovazzo, G. Polidori, R.
6 Spagna. *J. Appl. Crystallogr.* 36 (2003) 1103 .
- 7 [37] G.M. Sheldrick, *SHELXL–97, Programs for Crystal Structure Analysis (Release 97-2)*,
8 University of Göttingen, Germany, 1997.
- 9 [38] M.N. Burnette, C.K. Johnson, *ORTEP III*, Report ORNL-6895, Oak Ridge National
10 Laboratory. Tennessee. USA, 1996.
- 11 [39] L.J. Farrugia, *J. Appl. Crystallogr.* 30 (1997) 565.
- 12 [40] L.J. Farrugia, *J. Appl. Crystallogr.* 32 (1999) 837–838.
- 13 [41] A.J. Downard, B.H. Robinson, J. Simpson, *Organometallics* 5 (1986) 1132–1140.
- 14 [42] H.H. Ohst, J.K. Kochi, *Inorg. Chem.* 25 (1986) 2066–2074.
- 15 [43] J.S. McKennis, E.P. Kyba, *Organometallic* 2 (1983) 1249–1251.
- 16 [44] M.K. Harb, J. Windhager, A. Daraosheh, H. Görls, L.T. Lockett, N. Okumura, D.H.
17 Evans, R.S. Glass, D.L. Lichtenberger, M. El-khateeb, W. Weigand. *Eur. J. Inorg. Chem*
18 (2009) 3414–3420.
- 19 [45] A. Orthaber, M. Karnahl, S. Tschierlei, D. Streich, M. Stein, S. Ott. *Dalton Trans.* 43
20 (2014) 4537–4549.
- 21 [46] A. Darchen, E.K. Lhadi, D. Grandjean, A. Mousser, H. Patin, *J. Organomet. Chem.* 342
22 (1988) C15–C19.

Table 1 Crystal data and refinement details for X-ray structure determination of complexes **2** and **3**

	Complex 2	Complex 3
Molecular formula	C ₂₄ H ₂₈ Fe ₂ O ₁₀ P ₂ S ₂	C ₂₁ H ₂₈ FeO ₇ P ₂ S ₂
Formula weight (g mol ⁻¹)	714,25	574,40
T(K)	293(2)	293(2)
Crystal system	Triclinic	Orthorhombic
Space group	P-1	Pcab
a (Å)	11.7332(6)	13,0590(5)
b (Å)	14.5531(6)	14,7910(5)
c (Å)	10.5775(6)	27,4550(5)
α (°)	103.35(5)	90
β (°)	101.02(3)	90
γ (°)	71.20(3)	90
Volume (Å ³)	1591.7	5303,09(29)
Z	2	8
Color	red	violet
ρ _{cal} (g cm ⁻³)	1.490	1.440
μ (cm ⁻¹)	11.91	8,84
θ _{min} - θ _{max}	1 – 25	1.5 – 26.4
Measured data	5559	63108
Reflections used	2304	5417
F ₀₀₀	721.9	2382.7
Radiation	MoKα(Graphite Monochromated)	MoKα(Graphite Monochromated)
Wave length (Å)	0.71073	0.71073
No. data with I > 2σ	3929	3595
number of parameters	380	317
R _{int}	0.040	0.0801
R ₁ (I > 2σ)	0.03446	0.0695
wR ₂	0.04570	0.1762
GOF	1.614	1.077

Table 2 Selected bond lengths (Å) and angles (°) in complexes **2** and **3**

Complex 2		Complex 3	
Bond lengths (Å)		Bond lengths (Å)	
Fe (1) - S (1)	2.2821(1)	Fe (1) - S (1)	2.1932(14)
Fe (1) - S (2)	2.2771(1)	Fe (1) - S (2)	2.1523(13)
Fe (1) - P (1)	2.1681(1)	Fe (1) - P (1)	2.1452(14)
Fe (1) - C (1)	1.7545(1)	Fe (1) - C (7)	1.740(5)
Fe (1) - C (2)	1.7659(3)	/	/
S (1) - C (5)	1.8179(3)	S (1) - C (8)	1.727(4)
S (2) - C (6)	1.8219(9)	S (2) - C (9)	1.736(4)
C (5) - C (6)	1.3273(5)	C (8) - C (9)	1.364(6)
/	/	Fe (1) - P (2)	2.1220(14)
Fe (2) - S (1)	2.2921(1)	/	/
Fe (2) - S (2)	2.2615(1)	/	/
Fe (2) - P (2)	2.1725(1)	/	/
Fe (2) - C (3)	1.7643(3)	/	/
Fe (2) - C (4)	1.7651(13)	/	/
Fe (1) - Fe (2)	2.4797(1)	/	/
Angles (°)		Angles (°)	
S (1)-Fe (1)-S (2)	78.95(1)	S (1)-Fe (1)-S (2)	88.10(4)
S (1)-Fe (1)-P (1)	100.11(1)	S (1)-Fe (1)-P (1)	89.04(5)
/	/	S (1)-Fe (1)-P (2)	95.87(5)
S (2)-Fe (1)-C (1)	89.86(1)	S (2)-Fe (1)-C (7)	87.38(14)
S (1)-Fe (1)-C (1)	160.73(1)	S (1)-Fe (1)-C (7)	170.47(15)
S (2)-Fe (1)-P (1)	103.77(2)	S (2)-Fe (1)-P (1)	144.05(5)
S (1)-C (5)-C (6)	116.14(1)	S (1)-C (8)-C (9)	119.1(3)
Fe (1)-S (1)-C (5)	101.98(1)	Fe (1)-S (1)-C (8)	106.66(15)
Fe (1)-S (2)-C (6)	102.61(1)	Fe (1)-S (2)-C (9)	107.95(14)
/	/	P (2)-Fe (1)-P (1)	98.20(5)
/	/	S (2)-Fe (1)-P (2)	117.74(5)
Fe (2)-Fe (1)-P (1)	150.57(1)	/	/
Fe (1)-Fe (2)-P (2)	149.98(1)	/	/
S (1)-Fe (2)-S (2)	79.06(1)	/	/
S (1)-Fe (2)-P (2)	103.59(2)	/	/
S (2)-Fe (2)-P (2)	99.31(1)	/	/
Fe (2)-Fe (1)-S (1)	57.37(1)		
Fe (2)-Fe (1)-S (2)	56.58(1)		

Table 3 Hydrogen bonds (Å) and angles (°) in complexes **2** and **3**

	D – H...A	D – H	H...A	D ...A	D – H...A
Complex 2	C11 – H4 ...O5 ⁽ⁱ⁾	0.99	2.36	3.261(2)	148
	C9 – H2 ...S2 ⁽ⁱⁱ⁾	1	2.99	3.246(6)	176
Complex 3	C19– H19...O7 ⁽ⁱⁱⁱ⁾	0.93	2.62	3.993(3)	125

Symmetry codes: (i) -x+1,-y+1,-z+1; (ii) -x,-y+1,-z+1. (iii) x,y-1/2,-z+1/2.

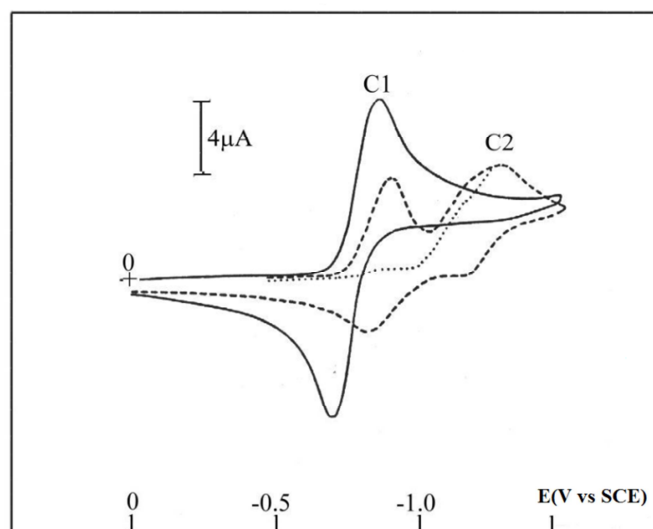


Fig.1. Cyclic voltammetry of 2 mM of complex **1** in CH_2Cl_2 0.1 M $\text{Bu}_4\text{N}^+\text{BF}_4^-$; Pt electrode; scan rate 0.1 V s^{-1} . — Complex **1** alone; ----- and First and second scan in the presence of an excess of $\text{P}(\text{OMe})_3$.

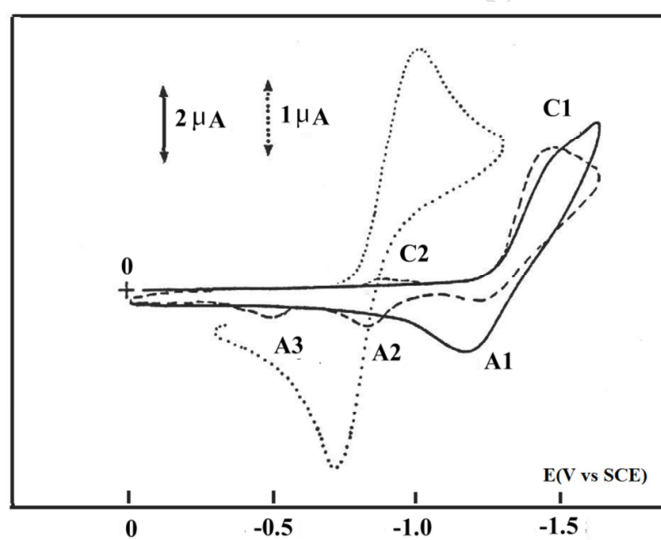


Fig.2. Cyclic voltammetry of 2 mM of complex **2** in CH_2Cl_2 0.1 M $\text{Bu}_4\text{N}^+\text{BF}_4^-$; Pt electrode; scan rate 0.2 V s^{-1} . — Complex **2** under N_2 atmosphere; ----- Complex **2** under CO atmosphere. Complex **1** (2 mM) under N_2 atmosphere.

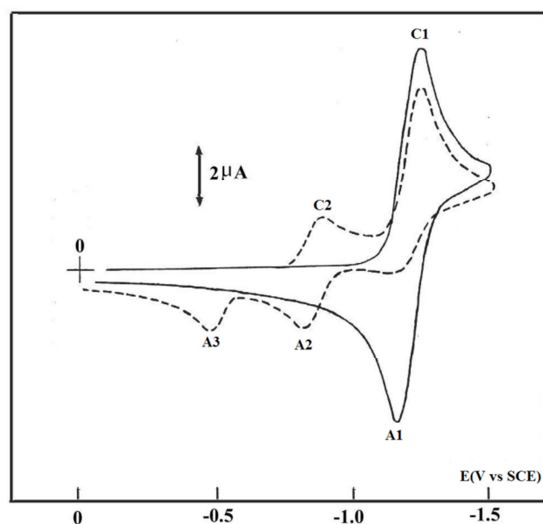


Fig.3. Cyclic voltammetry of 2 mM of complex **3** in CH_2Cl_2 0.1 M $\text{Bu}_4\text{N}^+\text{BF}_4^-$; Pt electrode; scan rate 0.2 V s^{-1} . — Complex **3** under N_2 atmosphere; Complex **3** under CO atmosphere.

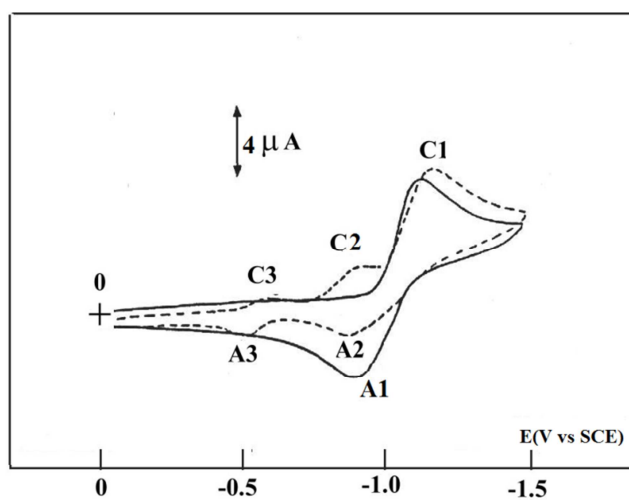


Fig.4. Cyclic voltammetry of 2 mM of complex **4** in CH_2Cl_2 0.1 M $\text{Bu}_4\text{N}^+\text{BF}_4^-$; Pt electrode; scan rate 0.2 V s^{-1} . — Complex **4** under N_2 atmosphere; Complex **4** under CO atmosphere.

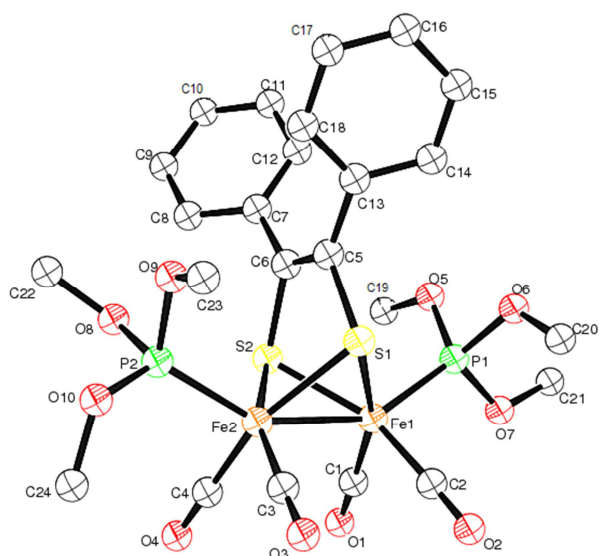


Fig.5. Molecular structure of complex **2** with thermal ellipsoids at 30% probability. Hydrogen atoms are omitted for clarity.

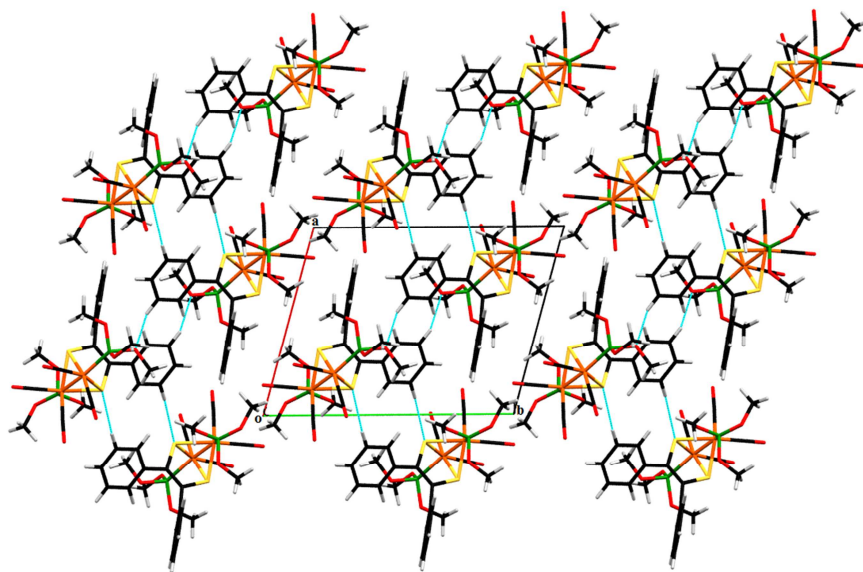


Fig.6. The crystal packing viewed along axis *c*. Dashed lines indicate intermolecular C–H...O and C–H...S hydrogen bonds which join molecules into endless chains along the *a*-axis direction.

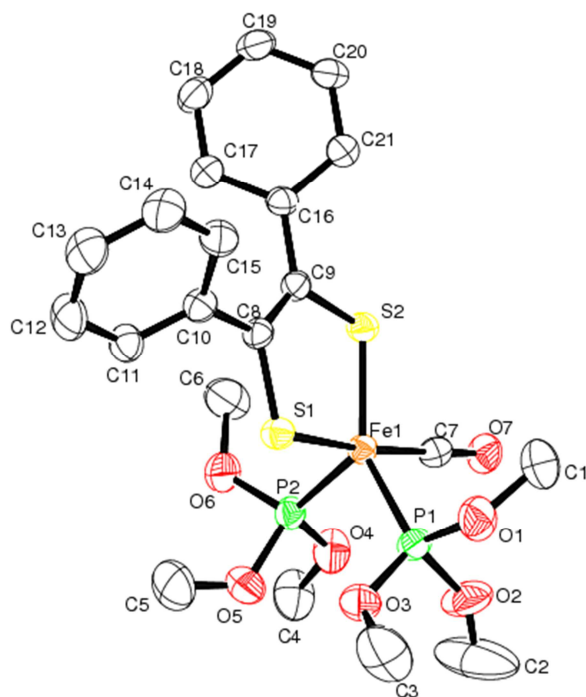


Fig.7. Molecular structure of complex **3** with thermal ellipsoids at 30% probability. Hydrogen atoms are omitted for clarity.

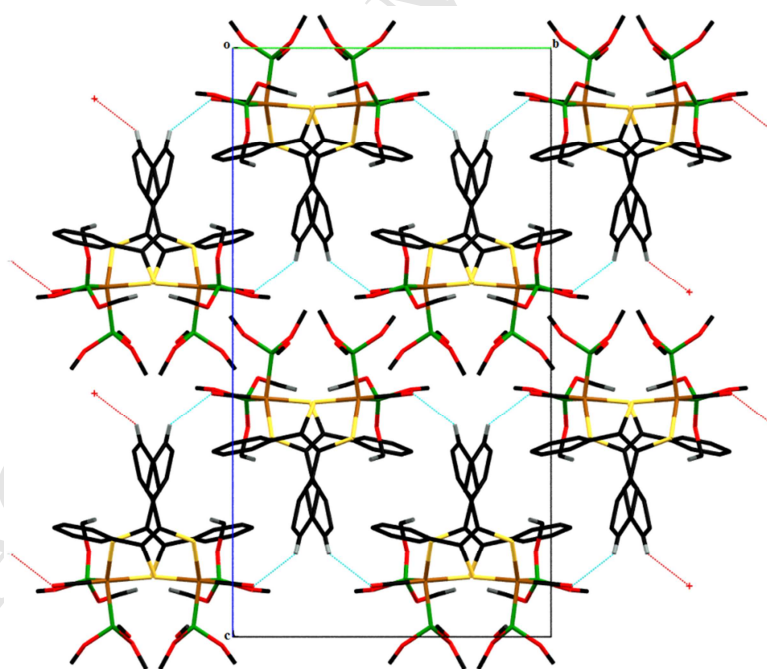
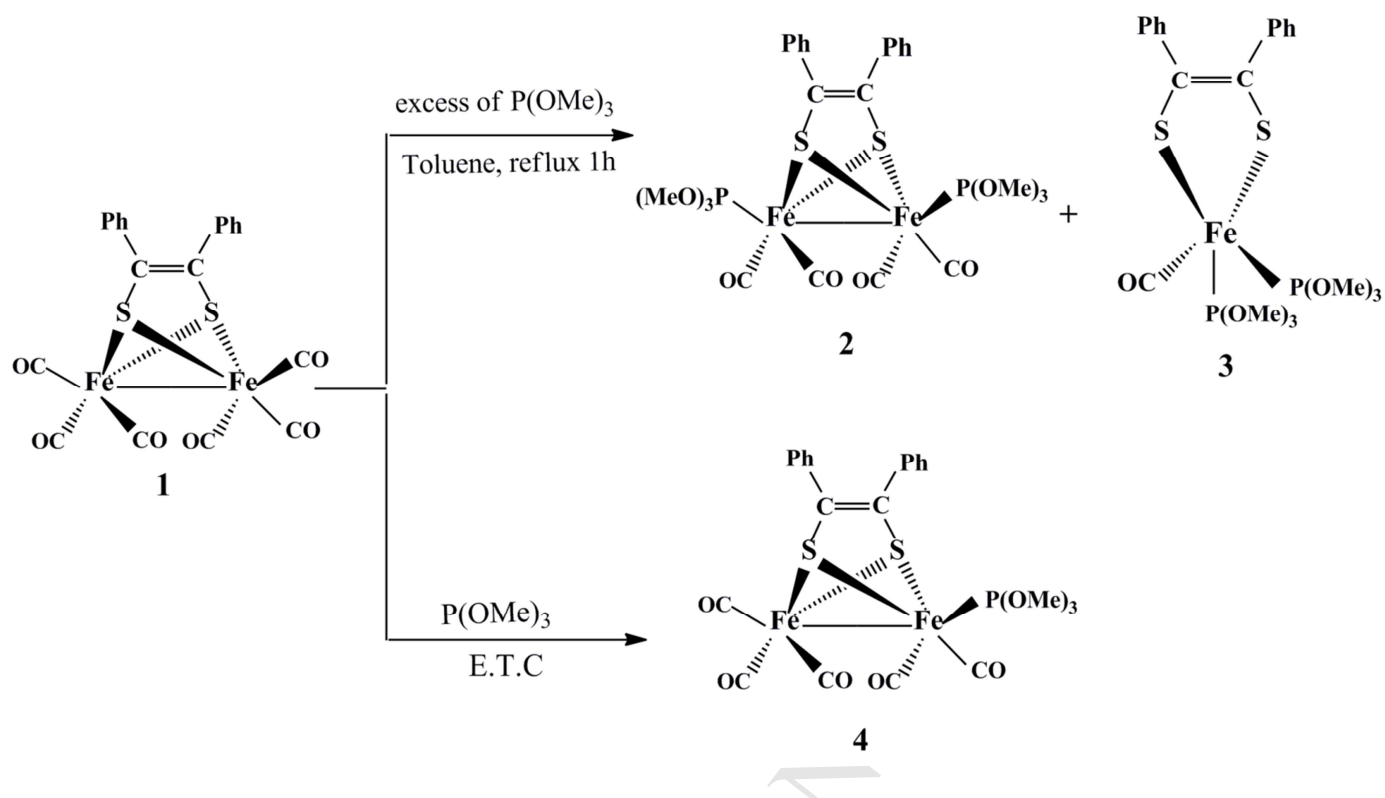
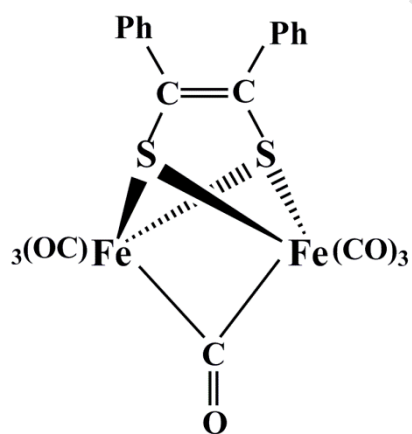


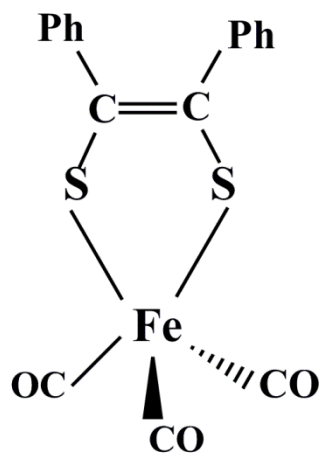
Fig.8. The crystal packing viewed along axis **a**. Dashed lines indicate C–H...O intermolecular hydrogen bond, forming a zigzag chain along the *b* axis at *c* = 0 and *c* = 1/2.



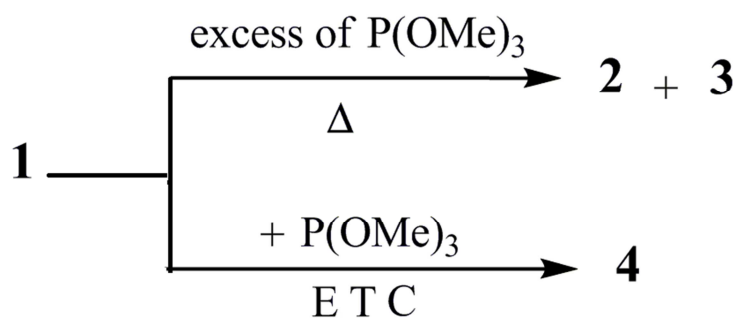
Scheme 1. Reaction under thermal and ETC activations



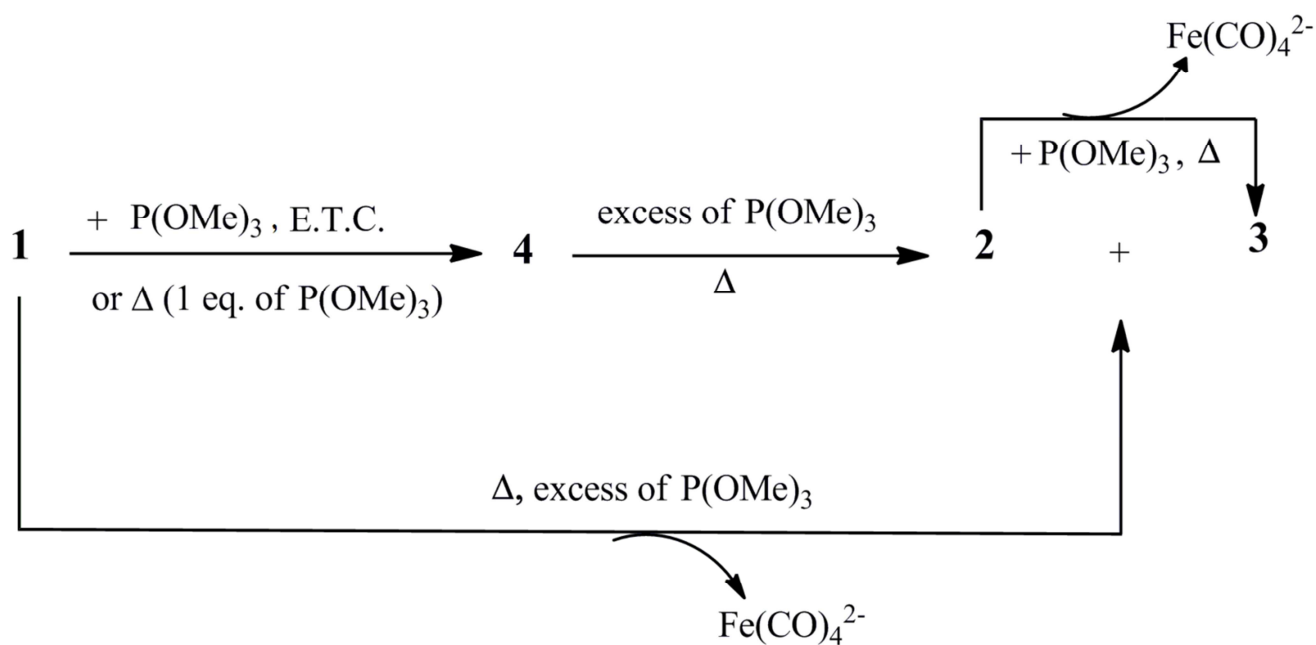
Scheme 2. Complex 5



Scheme 3. Complex 6



Scheme 4. Reactions of complex **1** with P(OMe)_3 under ETC and thermal activations



Scheme 5. Proposed mechanism of reaction of **1** with P(OMe)_3

- Carbonyl exchange by $\text{P}(\text{OMe})_3$ in $(\mu\text{-}\eta^2\text{PhC}(\text{S})=\text{C}(\text{S})\text{Ph})\text{Fe}_2(\text{CO})_6$ lead to three complexes
- Thermal activation lead to a binuclear and a mononuclear iron disubstituted complexes
- Under electron transfer catalysis a binuclear monosubstituted complex was obtained
- Complexes voltammetry showed a chemical two electrons reversible reduction step
- When $\text{P}(\text{OMe})_3$ was added CO substitutions were induced by electron transfer catalysis